Late Age- and Dose-Related Effects on the Proteome of Thyroid Tissue in Rats after ^{131}I Exposure

Malin Druid *, Emman Shubbar, Johan Spetz, Toshima Z Parris, Britta Langen, Charlotte Ytterbrink, Evelin Berger, Khalil Helou, Eva Forssell-Aronsson

Posted Date: 22 March 2024

doi: 10.20944/preprints202403.1345.v1

Keywords: Biomarker; low-dose exposure; ionizing radiation; radiobiology; proteomics; long-term effects; dose dependence

Article

Late Age- and Dose-Related Effects on the Proteome of Thyroid Tissue in Rats after ^{131}I Exposure

Malin Druid [1,*], Emman Shubbar [1], Johan Spetz [1], Toshima Z. Parris [2], Britta Langen [3], Charlotte Ytterbrink [1] Evelin Berger [4], Khalil Helou [2] and Eva Forssell-Aronsson [1,2]

1 Departments of [1]Medical Radiation Sciences and [3]Oncology, Institute of Clinical Sciences, Sahlgrenska Center for Cancer Research, Sahlgrenska Academy, University of Gothenburg, SE-413 45 Gothenburg, Sweden
2 Department of Medical Physics and Biomedical Engineering, Sahlgrenska University Hospital, SE-413 45 Gothenburg, Sweden
3 Section of Molecular Radiation Biology, Department of Radiation Oncology, University of Texas Southwestern Medical Center, Dallas, TX 75390, USA
4 Proteomics Core Facility, Sahlgrenska Academy, University of Gothenburg, SE-413 45 Gothenburg, Sweden
* Correspondence: malin.druid@regiondalarna.se

Summary: Thyroid diseases are commonly treated with ^{131}I due to the physiological uptake of iodine in thyroid tissue. Children are in general more sensitive compared to adults, and an increased number of thyroid malignancies were seen in children but not in adults after the Chernobyl accident. However, the long-term radiobiological mechanisms and response in is widely unknown. Thus, there is a need to increase the knowledge of these effects and identify if there is differences between children and adults.

Abstract: The physiological process of iodine uptake in the thyroid is used for ^{131}I treatment of thyroid diseases. Children are more sensitive to radiation compared to adults and may react differently to ^{131}I exposure. The aims of this study were to evaluate the effects on thyroid protein expression in young and adult rats one year after ^{131}I injection, and identify potential biomarkers related to ^{131}I exposure, absorbed dose, and age. Twelve Sprague Dawley Rats (young and adults) were i.v. injected with 50 kBq or 500 kBq ^{131}I and were killed twelve months later. Twelve untreated rats were used as age-matched controls. Quantitative proteomics, statistical analysis and evaluation of biological effects was performed. The effects of irradiation were most prominent in young rats. Protein biomarker candidates were proposed related to age, absorbed dose, thyroid function and cancer and a panel was proposed for ^{131}I exposure. In conclusion, the proteome of rat thyroid was differentially regulated twelve months after low-intermediate dose exposure to ^{131}I in both young and adult rats. Several biomarker candidates are proposed for ^{131}I exposure, age, and many of them are known to be related to thyroid function or thyroid cancer. Further research on human samples are needed for validation.

Keywords: biomarker; low-dose exposure; ionizing radiation; radiobiology; proteomics; long-term effects; dose dependence

1. Introduction

To maintain normal body function, the thyroid is essential for various cellular processes in different tissues [1]. The thyroid produces the T4 and T3 thyroid hormones that are important early in life, and an underproduction of thyroid hormone is associated with, for example, mental retardation and decreased length growth. However, overproduction of these hormones is associated with difficulties in controlling muscle function and increased length growth [2]. In addition, both types of malfunction (increased or decreased) can lead to cardiovascular issues [2]. The thyroid

 doi:10.20944/preprints202403.1345.v1

hormones are also needed to maintain normal metabolism during an individual's lifetime [3], and hypo- and hyperthyroidism are functional disorders that are vital to treat. Since the thyroid hormones contain iodine, physiological uptake of iodine occurs in the thyroid.

Several studies have shown that exposure to ionizing radiation can affect thyroid cellular function, primarily at higher absorbed doses, either by external (X-ray, gamma radiation) or internal irradiation (alpha particles, electrons) [4–7]. Irradiation of the thyroid can lead to, for example, hypothyroidism and thyroid cancer depending on several important factors including dose, dose rate, and type of irradiation [4–7]. This was seen by the increased incidence of thyroid cancers among children but not adults after the Chernobyl accident due to ^{131}I irradiation [8–13]. The acute effects (hours to weeks) of ^{131}I irradiation on, e.g. organ functions are most important for high absorbed doses, while long-term effects (months to years) are also important for low absorbed doses. Late effects of ^{131}I exposure are also of importance after cancer treatment with ^{131}I-labelled radiopharmaceuticals, e.g. ^{131}I-MIBG therapy of neuroblastoma in children and pheochromocytoma and paraganglioma in adults [14,15]. These effects are functional changes in ^{131}I avid tissues, such as thyroid and salivary glands, but also risk of secondary cancer induction.

We still have limited knowledge of the long-term effects of radiation, especially for low absorbed doses. Radiation-induced biomarkers *e.g.* proteins would enable us to evaluate and eventually predict the effects of exposure to ionizing radiation [14,16]. We have previously proposed several biomarker candidates from mouse and rat thyroid tissue after ^{131}I injection. For short-term effects (24 h after injection): the *Agpat9, Klk1,* the *Klk1b* family, *Plau, Prf1, S100a8* transcripts were suggested. For long-term effects (three to nine months after injection) we identified the following groups of transcripts and proteins: a) exposure-related: the *Afp* and *RT1-Bb* transcripts and the ARF3, DLD, IKBKB, NONO, RAB6A, RPN2, SLC25A5, PTH, KRT13, and eEF1A1 proteins, b) dose-related: the APRT, LDHA, TGM3, and DSG4 proteins, and c) thyroid function-related: the *Vegfb* transcript, the ACADL, SORBS2, TPO and TG proteins [17–20].

The aim of this study was to identify protein biomarker candidates in thyroid tissue for long-term effects (12 months) of radiation exposure, absorbed dose, and age at exposure in young and adult rats irradiated with low to moderate absorbed doses of ^{131}I. Further, their relationship to thyroid function and thyroid cancer were discussed.

2. Material and Methods

2.1. Rat Model

This study was performed on 36 healthy Sprague Dawley rats (Charles River; Germany). The animals had free access to food and water and were under daily supervision. The study was approved by the Ethical Committee on Animal Experiments in Gothenburg, Sweden (Permit Number: 145-2015).

Twelve five-week-old rats, representing young rats, were i.v. injected with 50 or 500 kBq ^{131}I (n=6/group), and six rats of the same age were mock treated with saline solution (controls). The remaining 18 rats (17 week old adults) were treated in a similar manner as the young rats (n=6/group). The absorbed dose to the thyroid after i.v. injection of 50 or 500 kBq ^{131}I was estimated to 0.1 and 1 Gy for young rats and 0.07 and 0.7 Gy for adult rats, respectively. These values were based on data from a previous dosimetric study, correcting for differences in thyroid mass, and assuming similar fraction of thyroidal uptake of ^{131}I [21,22].

Twelve months after ^{131}I injection, the rats were killed by cardiac puncture after a pentabarbitalnatrium injection (APL; Kungens kurva, Sweden). Thyroid tissue was surgically removed from each rat and each divided into two pieces, one was flash-frozen in liquid nitrogen and the other was fixed in formalin and imbedded in paraffin for histological analysis. A certified pathologist evaluated thyroid tissue morphology, abnormal tissue structure, and the presence of tumour cells, using paraffin sections (4 μm) stained with haematoxylin and eosin.

 doi:10.20944/preprints202403.1345.v1

2.2. Mass Spectrometry Analysis of Proteins

2.2.1. Protein Extraction, Digestion and TMT-Labelling

The samples were homogenised using the lysis matrix D on FastPrep®-24 instrument (MP Biomedicals, OH) in lysis buffer (50 mM triethylammonium bicarbonate (TEAB), 2% sodium dodecyl sulfate (SDS)) and 5 cycles 40 s each. The samples were centrifuged at maximum speed for 15 min and the supernatant was transferred to a new vial and washed with the lysis buffer, followed by centrifugation at maximum speed. The supernatants were combined and protein concentration was determined using Pierce™ BCA Protein Assay (Thermo Scientific) and the Benchmark Plus microplate reader (BIO-RAD) with BSA solutions as standards. A representative reference containing equal amounts from each group were made.

Aliquots containing 30 µg from each protein extraction were digested with trypsin using the filter-aided sample preparation (FASP) method [23]. Briefly, samples were reduced with 100 mM dithiothreitol at 60°C for 30 min, transferred to 30 kDa MWCO Pall Nanosep centrifugation filters (Sigma-Aldrich), washed repeatedly with 8 M urea and once with digestion buffer prior (1% sodium deoxycholate (SDC) in 50 mM TEAB) to alkylation with 10 mM methyl methanethiosulfonate in digestion buffer for 30 min. Digestion was performed in digestion buffer by addition of 0.5 µg Pierce MS grade Trypsin (Thermo Fisher Scientific) at 37°C and incubated overnight. Additional trypsin was added and incubated for another two hours. Peptides were collected by centrifugation.

Digested peptides were labeled using TMT 10-plex isobaric mass tagging reagents (Thermo Scientific) according to the manufacturer instructions. Samples were randomised across the four TMT-sets containing also one reference each. Sodium deoxycholate was removed by acidification with 10% TFA. The combined sets were pre-fractionated into 40 fractions with basic reversed-phase chromatography (bRP-LC) using a Dionex Ultimate 3000 UPLC system (Thermo Fischer Scientific). Peptide separations were performed using a reversed-phase XBridge BEH C18 column (3.5 µm, 3.0x150 mm, Waters Corporation) and a linear gradient from 3% to 40% solvent B over 18 min followed by an increase to 100% B over 5 min. Solvent A was 10 mM ammonium formate buffer at pH 10.00 and solvent B was 90% acetonitrile, 10% 10 mM ammonium formate at pH 10.00. The fractions were concatenated into 20 fractions (1+21, 2+22, …, 20+40), dried and reconstituted in 3% acetonitrile, 0.2% formic acid.

2.2.2. Nano Liquid Chromatography Tandem Mass Spectrometry (nLC-MS/MS)

The labelled peptide fractions were analysed by an Orbitrap Fusion™ Lumos™ Tribrid™ mass spectrometer interfaced with Easy-nLC1200 liquid chromatography system (Thermo Fisher Scientific). Peptides were trapped on an Acclaim Pepmap 100 C18 trap column (100 µm x 2 cm, particle size 5 µm, Thermo Fisher Scientific) and separated on an in-house packed analytical column (75 µm x 30 cm, particle size 3 µm, Reprosil-Pur C18, Dr. Maisch) using a linear gradient from 5% to 33% B over 77 min followed by an increase to 100% B for 3 min, and 100% B for 10 min at a flow of 300 nL/min. Solvent A was 0.2% formic acid and solvent B was 80% acetonitrile, 0.2% formic acid. Precursor ion mass spectra were acquired at 120 000 resolution and MS/MS analysis was performed in a data-dependent multinotch mode where CID spectra of the most intense precursor ions were recorded in ion trap at collision energy setting of 35% for 3 s ('top speed' setting). Precursors were isolated in the quadrupole with a 0.7 m/z isolation window, charge states 2 to 7 were selected for fragmentation, dynamic exclusion was set to 45 s and 10 ppm. MS^3 spectra for reporter ion quantitation were recorded at 50 000 resolution with HCD fragmentation at collision energy of 65 using the synchronous precursor selection.

2.2.3. Proteomics Data Analysis

The generated data files for each set were merged for identification and relative quantification using Proteome Discoverer version 2.2 (Thermo Fisher Scientific). The search was against Uniprot *Rattus norwegicus* (app. 38,000 sequences) using Mascot version 2.5.1 (Matrix Science) as a search

 doi:10.20944/preprints202403.1345.v1

engine. The precursor mass tolerance was set to 5 ppm and fragment mass tolerance to 0.6 Da. Tryptic peptides were accepted with zero missed cleavage, variable modifications of methionine oxidation and fixed cysteine alkylation, TMT-label modifications of N-terminal and lysine were selected. The reference samples were used as denominator during calculation of the ratios of protein abundances. Percolator was used for the validation of identified proteins. TMT reporter ions were identified in the MS3 HCD spectra with 3 mmu mass tolerance, and the TMT reporter intensity values for each sample were normalised on the total peptide amount. The quantified proteins were filtered at 5% FDR and grouped by sharing the same sequences to minimise redundancy. Unique peptides for a given protein were considered for quantification of the proteins. The mass spectrometry proteomics data have been deposited to the ProteomeXchange Consortium via the PRIDE [24] partner repository with the dataset identifier PXD024786.

2.3. Statistical Analysis of Protein Expression Data

Protein expression was compared between exposed and non-exposed groups. Log2 ratios were calculated by dividing corresponding logarithmised protein expression values (50kBq or 500kBq divided by control). A two-fold upregulation is hence a value of 1, whereas a two-fold downregulation results in a value of -1.

The Perseus 1.6.7.0 software was used for statistical analysis. The proteins that appeared in less than three of the replicates were discharged. The fold change value was calculated using geometrical mean value and was log2 transformed. Statistical significant protein regulation was determined using Anova test ($p<0.05$). To find proteins that were statistical significant between different groups Welsh t-tests ($p<0.05$) were performed. The log2 ratio cut off was set to >0.58 and <-0.58. A heat map was generated in Perseus, using the "Heretical clustering" function on the statistically significant proteins.

2.4. Ingenuity Pathway Analysis

Ingenuity Pathway Analysis (IPA; Ingenuity Systems) was used to identify and analyse canonical pathways, biological functions and diseases as well as upstream regulators related to the identified proteins. To establish statistical significance, Fisher´s exact test ($p<0.05$) was used. The bias corrected z-value cut off was set to ±2 to denote activation or inhibition, respectively.

3. Results

Hereafter, the groups are denoted A for adult, Y for young, 50 for 50 kBq and 500 for 500 kBq ^{131}I activity. Hence, the group names are denoted A50, A500, Y50, and Y500.

In total, 7.147 proteins were quantified using nLC-MS/MS in thyroid tissue from exposed *versus* non-exposed rats. Of these, 1,799 significantly regulated proteins compared to controls with a log2 ratio >0.58 or <-0.58 where identified. The majority of the identified proteins affected were down-regulated and to a moderate extent (-0.58-(-4.5) log2 ratio), and only a few proteins were up-regulated (0.58-4.5) log2 ratio) (Figure 1). The young rats had fewer clusters in common compared to adult rats, which had a larger similarity of clusters. Of the 1,799 significant proteins, 758 were identified in only one of the groups and the remaining 1,041 proteins were identified in at least two groups (Figure 2). Interestingly, 24 proteins were identified in all groups (exposure-related, but not dose-related), all of which showed decreased expression levels, except timeless circadian regulator (TIMELESS) that displayed elevated expression in the A500 group (Figure 3).

 doi:10.20944/preprints202403.1345.v1

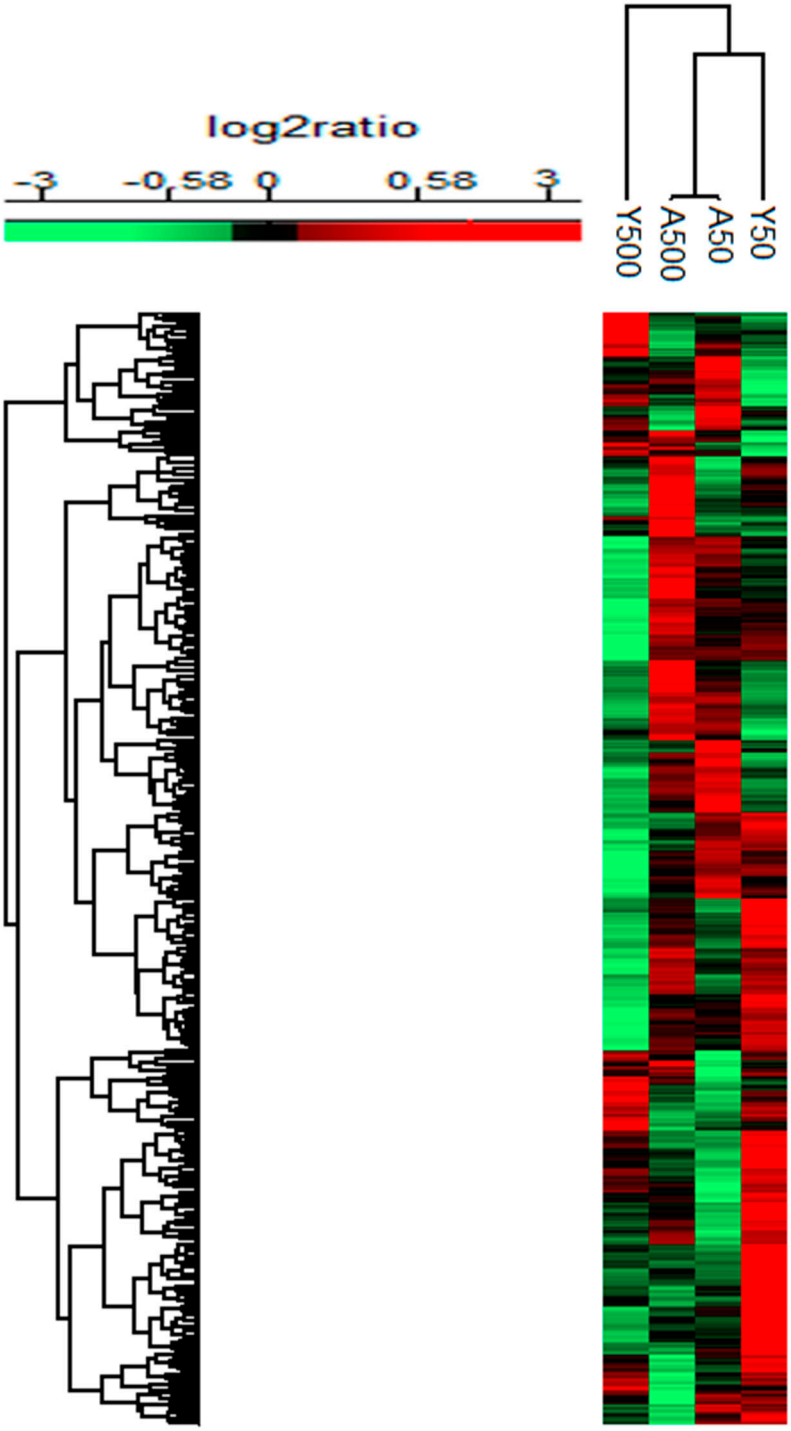

Figure 1. Heat map for the significantly regulated proteins with a log2 ratio >0.58 or <-0.58 and p-value <0.05 after ^{131}I exposure (injection of 50 or 500 kBq ^{131}I) of young and adult rats compared to age matched non-exposed rats. Upregulation is represented in red, and downregulation in green colour.

Preprints.org (www.preprints.org) | NOT PEER-REVIEWED | Posted: 22 March 2024 doi:10.20944/preprints202403.1345.v1

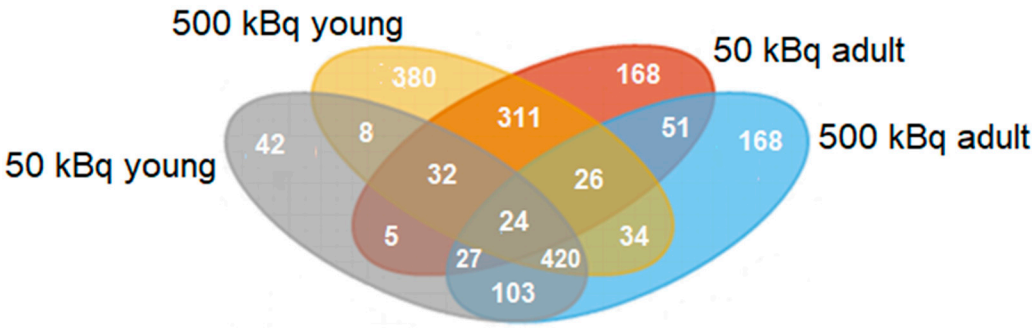

Figure 2. Venn diagram for the significantly regulated proteins after ^{131}I exposure (injection of 50 or 500 kBq ^{131}I) of young and adult rats compared to age matched non-exposed rats. The 50 kBq young rat group (Y50) is represented in grey, 500 kBq young (Y500) is represented in yellow, 50 kBq adult (A50) is represented in red, and 500 kBq adult (A500) is represented in blue.

Proteins	Y50	Y500	A50	A500	Proteins	Y50	Y500	A50	A500
ADAT2					MINDY2				
ANXA9					MYLK4				
BOK					NADSYN1				
CRTC3					NOC2L				
CTR9					RGD1563056				
DAAM2					RNF121				
DNM1					RNGTT				
DYNLT1					SLC9A7				
ENY2					SMIM7				
IPO11					ST5				
LOC100909677					TIMELESS				
MBLAC1					TMEM98				

Figure 3. The 24 proteins that were in common for all four groups. All the proteins, but TIMELESS had decreased expression for all groups. A log2ratio between -0.58-(-1.0), -1.0-(-1.5), -1.5-(-2.0) and 0.58-1.0 is marked in light blue, blue, dark blue and red respectively.

3.1. Group-Specific (Unique) Proteins

Compared to the controls, 758 proteins were differentially expressed in only one of the groups, i.e. 42, 380, 168, and 168 proteins for the Y50, Y500, A50, and A500, respectively (Suppl. Table S1). Higher log2 ratio were generally seen for the proteins identified in the groups exposed to 500 kBq of ^{131}I. The top ten differentially expressed proteins with the highest increased and decreased expression for each group were identified (Figure 4). Of these 40 proteins, eight proteins had a log2 ratio below -1.5 and six proteins had a log2 ratio above 1.5. The following proteins had a log2 ratio in the interval -1.5-(-2): cytochrome P450 family 2 subfamily U member 1 protein (CYP2U1; Y500), enoyl-CoA delta isomerase 2 (ECI3; Y500), alcohol dehydrogenase 1 (ADH1; Y500), arylformamidase (AFMID; Y500), myosin heavy chain (MYHC; A50), Rh blood group D antigen (RHD; A50), potassium inwardly rectifying channel subfamily J member 16 (KCNJ16; A500), and PPARGC1 and ESRR induced regulator, muscle 1 (PERM1; A500). The proteins with a log2 ratio in the interval 1.5-2 were: adenosine deaminase (ADA; Y500), hornerin (HRNR; Y500), myosin XVIIIB (MYO18B; A500), and kininogen 1 (KNG1; A500). The myosin heavy chain 8 (MYH8; Y500) and repetin (RPTN; Y500) proteins had a log2 ratio in the interval 2-4.

 doi:10.20944/preprints202403.1345.v1

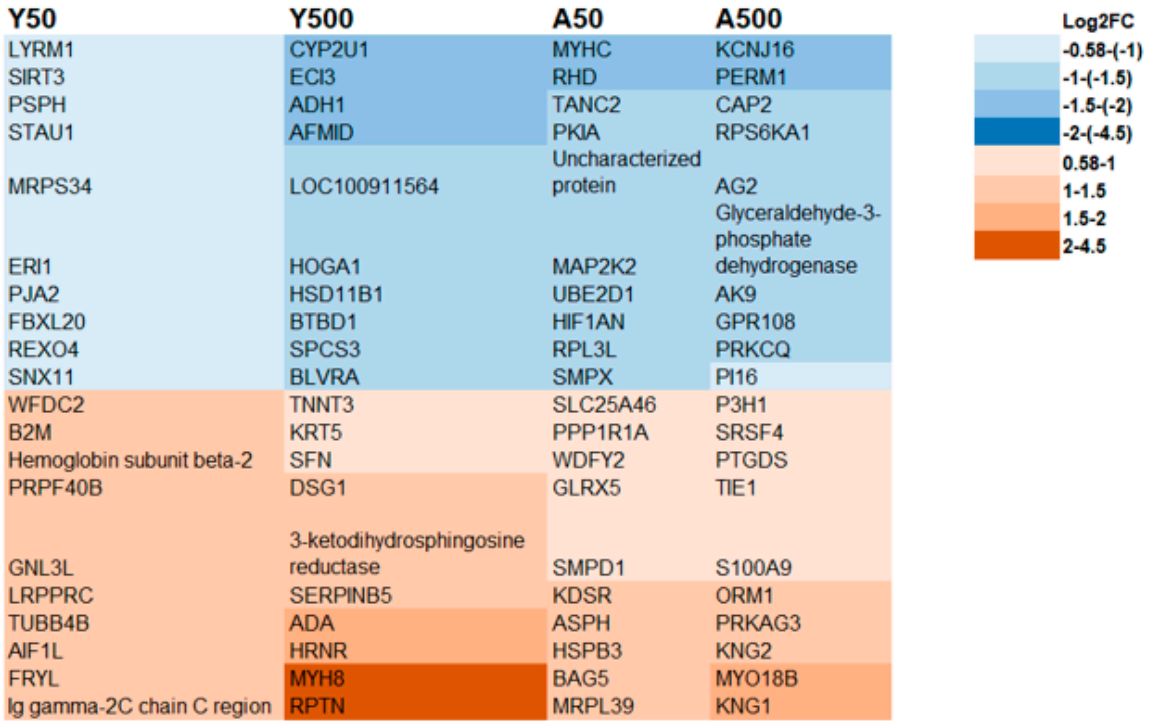

Figure 4. The top 10 significantly regulated unique proteins for each group with the highest decreased (blue) or increased (brown) expression levels. A trend of higher expression was seen for the 500 kBq groups compared to the 50 kBq groups.

3.2. Age-Related Proteins

In total, 59 significantly regulated proteins were found in only young or adult rats, irrespective of amount of ^{131}I activity level, i.e. 8 were detected in young and 51 in adult individuals (Figure 2 and Table 1). All proteins seen in young individuals had decreased expression levels. Furthermore, 39 of the 51 proteins seen in adults had decreased expression, ten had increased expression in both groups (A50 and A500), and two had decreased expression in A50 and increased expression in A500. For the Y50 and A50 groups, 42 and 168 unique proteins were regulated, respectively. The corresponding numbers of unique proteins were 380 and 168 for the Y500 and A500 groups, respectively (Suppl. Table 1).

Table 1. Age-related proteins in common for young and adult rats, respectively, irrespective of ^{131}I activity injected. In total, eight proteins were significantly down-regulated in young individuals. For the adults, 51 proteins were significantly regulated, the majority of which were down-regulated.

Young		Adult			
Protein	**Log2 ratio (Y50; Y500)**	**Protein**	**Log2 ratio (A50; A500)**	**Protein**	**Log2 ratio (A50; A500)**
FDPS	-0.60; -0.72	AHNAK 1 (Fragment)	-0.66; -0.72	LCN2	0.98; 0.69
GNPTAB	-0.63; -0.66	ALDH1A7	1.3; 1.0	LGALS5	0.89; 2.0
JAK1	-0.63; -0.69	APOBEC2	1.1; 0.88	NCAPG2	-1.1; -0.69
LSAMP	-0.59; -0.82	APOD	--1.3; -0.81	NHSL1	-0.85; -1.1
MAOB	-0.61; -0.73	ATPSCKMT	0.81; 0.63	NR2F2	-0.93; -0.75
REEP6	-0.58; -0.96	BLOC1S6	-0.82; -0.97	PATZ1	-0.64; -0.92
RGD1566265	-0.60; -1.0	BUD23	-1.1; -1.4	PDLIM4	-0.73; -0.61
TBC1D10A	-0.66; -0.65	CACNG1	-1.8; -1.2	PHKG2	-0.59; -0.63
		COX3	-0.85; -1.1	PISD	-0.68; -0.65
		CSTF1	-0.73; -0.74	PLSCR1	-0.86; -0.73
		DHRS7B	-1.2; -0.61	PPP1R10	-0.96; -0.99

 doi:10.20944/preprints202403.1345.v1

DNAH6	-0.59; -1.6	PRR33	1.9; 1.4
DPH6	-1.4; -2.1	PSMB8	1.8; 1.2
DVL1	-0.62; -0.93	RAC2	-0.68; -0.61
ECI1	-1.3; 0.90	RB1	-1.1; -0.62
FBXW17	-0.65; -1.0	RT1-A1B	4.4; 1.4
FCGBP	-0.83; -0.78	SNPH	-1.0; -0.82
FXYD1	--0.99; -0.59	TAP2	-0.59; -1.0
HAT1	-0.67; -0.63	TAP2C	1.5; 1.3
IGFBP6	--0.69; -0.65	TFE3	-0.59; 0.99
IGHG	0.67; 0.71	Titin protein homolog (Fragment)	-1.3; -0.60
KRT1	-1.0; -0.97	TMEM47	-0.63; -0.58
KRT10	-1.1; -0.83	TPCR12	-0.94; -1.2
KRT16	-1.6; -1.4	TXLNB	-2.0; -1.9
KRT80	-0.65; -0.70	Uncharacterized protein	-1.9; -1.7
LAMC2	-0.76; -0.69		

3.3. Dose-Related Proteins

Thirty-nine unique proteins were significantly regulated for the different doses (50 and 500 kBq), irrespective of age at exposure, i.e. 5 for the 50 kBq groups (unique for Y50 and A50) and 34 for the 500 kBq groups (unique for Y500 and A500; Figure 2 and Table 2). Of these, 3 had increased expression, 29 had decreased expression, and 7 had increased expression in young and decreased expression in adult rats.

Table 2. Dose-related proteins for an injected ^{131}I activity of 50 or 500 kBq, irrespective of age. Five significant proteins were seen in the 50 kBq groups and 34 in the 500 kBq group.

50 kBq		**500 kBq**			
Protein	**Log2 ratio (young; adult)**	**Protein**	**Log2 ratio (young; adult)**	**Protein**	**Log2 ratio (young; adult)**
BICD2	-0.62; -0.59	ABCC8	-1.1; -0.90	MEF2D	-0.67; -0.70
HABP4	-0.61; -0.63	ADGRG2	-0.98; -0.78	MOCOS	-1.1; -0.68
HBB-B1	0.65; -0.71	ALDH1A2	-0.65; -0.66	MTM1	-0.85; -0.88
NME3	0.60; 2.0	BHMT	-2.7; -0.77	MYL3	1.6; -0.73
PALM2	0.63; 0.70	CDC40	-1.1; -0.84	PKP1	1.2; -1.1
		CLCC1	0.84; 1.0	PRKCZ	-0.79; -0.62
		CNST	-0.62; -1.3	PSMF1	-0.95; -0.66
		CPT2	1.1; 0.90	RBM3	-0.64; -1.86
		CSRP3	0.99; -0.73	SERPINB12	3.1; -0.64
		DAB2	-0.81; -0.74	SLC25A15	-0.89; -0.74
		DNAJC17	-0.60; -0.69	SMPD3	1.5; -2.9
		DUSP22	-1.1; -0.69	THBS4	0.72; -1.0
		FLT4	-0.88; -1.3	TMEM106B	-1.2; -1.3
		HEG1	-0.72; -0.60	TP53I11	-0.77; -1.1
		HP	0.87; 0.74	UBAC1	-0.78; -0.82
		IGSF8	-0.89; -0.80	VASN	-1.1; -0.78
		LEAP2	-1.0; -0.85	WIZ	-0.67; -0.94

3.4. IPA Analysis

Using the 1,799 significantly regulated proteins, the canonical pathway analysis resulted in the identification of 37 statistically significant pathways (Table 3). The vast majority of these pathways

 doi:10.20944/preprints202403.1345.v1

were seen in young rats, with 18 and 15 for Y50 and Y500 groups, respectively. Few canonical pathways related to signalling were significant in the adult groups, i.e. one in the A50 group (Xenobiotic metabolism CAR signalling pathway) and three in the A500 group (IKL signalling, apelin cardiomyocyte signalling pathway and actin cytoskeleton signalling). Altogether, four upstream regulators were identified, where none was found in the Y50 group, ephrin A2 (EFNA2) in the Y500 group, lethal-7 miRNA (let-7) and insulin-like growth factor 1 (IGF1) in the A50 group, and myocardin (MYOCD) in the A500 group (Table 4).

Table 3. Ingenuity canonical pathway analysis using the IPA software. The vast majority of obtained pathways were seen in young individuals and only a few were found in adult rats.

Ingenuity canonical pathways	p	z	Molecules
Y50			
tRNA Splicing	1.7E-02	2.0	PDE10A,PDE1B,PDE5A,TSEN2
Stearate Biosynthesis I (Animals)	2.5E-02	-2.0	CYP2E1,DHCR24,GNPAT,SLC27A5
Superpathway of Methionine Degradation	1.0E-02	-2.0	BHMT,BHMT2,CTH,MAT1A
Thyroid Hormone Metabolism II (via Conjugation and/or Degradation)	7.4E-03	-2.0	SULT1B1,UGT1A1,Ugt2b17,UGT2B28
Gluconeogenesis I	1.4E-03	-2.0	ALDOB,ENO3,FBP1,PGAM2
Glycolysis I	2.6E-04	-2.2	ALDOB,ENO3,FBP1,PGAM2,PKLR
Bile Acid Biosynthesis, Neutral Pathway	7.9E-06	-2.2	AKR1D1,BAAT,CYP27A1,CYP3A4,SLC27A5
Xenobiotic Metabolism PXR Signaling Pathway	3.7E-06	-2.5	ALDH1L1,ALDH1L2,ALDH8A1,CAMK2G,CYP2C19,CYP2C9,CYP3A4,GSTA5,MAOB,PPP1R11,PRKCE,SULT1B1, SULT1E1,UGT1A1,UGT2B28,UGT8
LPS/IL-1 Mediated Inhibition of RXR Function	1.2E-07	2.6	ACOX2,ALDH1L1,ALDH1L2,ALDH8A1,CPT2,CYP2A6 (includes others),CYP2C19,CYP2C9,CYP3A4,Cyp4a14, FABP1,ABP3,FMO4,GSTA5,HMGCS2,MAOB,MYD88,SLC27A5,SULT1B1,SULT1E1
Serotonin Degradation	4.3E-04	-2.6	ADH1C,ADH4,MAOB,SULT1B1,UGT1A1,Ugt2b17,UGT2B28
Acetone Degradation I (to Methylglyoxal)	4.0E-06	-2.6	CYP2A6 (includes others),CYP2C18,CYP2C19,CYP2C9, CYP2E1,CYP2U1,CYP3A4
Bupropion Degradation	9.8E-07	-2.6	CYP2A6 (includes others),CYP2C18,CYP2C19,CYP2C9, CYP2E1,CYP2U1,CYP3A4
Xenobiotic Metabolism CAR Signaling Pathway	1.4E-05	-2.8	ALDH1L1,ALDH1L2,ALDH8A1,Cyp2b13/Cyp2b9,CYP2C19,CYP2C9,CYP3A4,FMO4,GSTA5,PRKCE,SULT1B1, SULT1E1, UGT1A1,UGT2B28,UGT8
Nicotine Degradation II	2.4E-08	-2.9	AOX1,CYP2A6 (includes others),CYP2C18,CYP2C19, CYP2C9,CYP2E1,CYP2U1,CYP3A4,FMO4,UGT1A1,Ugt2b17, UGT2B28
Estrogen Biosynthesis	2.5E-07	-3,0	CYP2A6 (includes others),CYP2C18,CYP2C19,CYP2C9, CYP2E1,CYP2U1,CYP3A4,HSD17B13,HSD17B2
Melatonin Degradation I	4.5E-08	-3.3	CYP2A6 (includes others),CYP2C18,CYP2C19,CYP2C9, CYP2E1,CYP2U1,CYP3A4,SULT1B1,UGT1A1,Ugt2b17, UGT2B28
Nicotine Degradation III	4.5E-08	-3.3	AOX1,CYP2A6 (includes others),CYP2C18,CYP2C19,

 doi:10.20944/preprints202403.1345.v1

			CYP2C9,CYP2E1,CYP2U1,CYP3A4,UGT1A1,Ugt2b17,UGT2B28
Superpathway of Melatonin Degradation	8.9E-09	-3.5	CYP2A6 (includes others),CYP2C18,CYP2C19,CYP2C9, CYP2E1,CYP2U1,CYP3A4,MAOB,SULT1B1,UGT1A1, Ugt2b17,UGT2B28
Y500			
Thyroid Hormone Metabolism II (via Conjugation and/or Degradation)	2.0E-03	-2.0	SULT1B1,UGT1A1,Ugt2b17,UGT2B28
Retinoate Biosynthesis I	1.8E-03	-2.0	ADH1C,ADH4,ALDH8A1,Rdh7
Noradrenaline and Adrenaline Degradation	1.6E-03	-2.0	ADH1C,ADH4,ADHFE1,MAOB
Superpathway of Cholesterol Biosynthesis	1.2E-03	-2.0	CYP51A1,DHCR24,FDPS,HMGCS2
Bile Acid Biosynthesis, Neutral Pathway	4.6E-05	-2.0	AKR1D1,BAAT,CYP3A4,SLC27A5
Citrulline Biosynthesis	8.3E-06	-2.0	ARG1,GLS,LOC102724788/PRODH,OTC
Superpathway of Citrulline Metabolism	3.0E-06	-2.2	ARG1,CPS1,GLS,LOC102724788/PRODH,OTC
Estrogen Biosynthesis	7.9E-13	-2.3	CYP2A6 (includes others),CYP2C18,CYP2C19,CYP2C9, CYP2E1,CYP2F1,CYP2S1,CYP2U1,CYP3A4,CYP51A1,HSD17B13,HSD17B2
Nicotine Degradation II	1.3E-12	-2.7	Aox3,CYP2A6 (includes others),CYP2C18,CYP2C19, CYP2C9,CYP2E1,CYP2F1,CYP2S1,CYP2U1,CYP3A4, CYP51A1,UGT1A1,Ugt2b17,UGT2B28
Melatonin Degradation I	1.3E-13	-2.7	CYP2A6 (includes others),CYP2C18,CYP2C19,CYP2C9, CYP2E1,CYP2F1,CYP2S1,CYP2U1,CYP3A4,CYP51A1, SULT1B1,UGT1A1,Ugt2b17,UGT2B28
Nicotine Degradation III	1.3E-13	-2.6	Aox3,CYP2A6 (includes others),CYP2C18,CYP2C19,CYP2C9, CYP2E1,CYP2F1,CYP2S1,CYP2U1,CYP3A4,CYP51A1, UGT1A1,Ugt2b17,UGT2B28
Serotonin Degradation	4.6E-06	-2.8	ADH1C,ADH4,ADHFE1,MAOB,SULT1B1,UGT1A1,Ugt2b17,UGT2B28
Superpathway of Melatonin Degradation	2.0E-14	-2.87	CYP2A6 (includes others),CYP2C18,CYP2C19,CYP2C9, CYP2E1,CYP2F1,CYP2S1,CYP2U1,CYP3A4,CYP51A1,MAOB, SULT1B1,UGT1A1,Ugt2b17,UGT2B28
Xenobiotic Metabolism CAR Signaling Pathway	1.3E-04	-3.3	ALDH1L2,ALDH8A1,Cyp2b13/Cyp2b9,CYP2C19,CYP2C9, CYP3A4,GSTA5,SULT1B1,SULT1E1,UGT1A1,UGT2B28
Xenobiotic Metabolism PXR Signaling Pathway	5.9E-06	-3.6	ALDH1L2,ALDH8A1,CAMK2A,CYP2C19,CYP2C9,CYP3A4, GSTA5,MAOB,Ppp1cc,SULT1B1,SULT1E1,UGT1A1,UGT2B28
A50			
Xenobiotic Metabolism CAR Signaling Pathway	3.9E-03	2.3	ALDH8A1,GSTA1,GSTA5,MAP2K2,MAP2K5,SULT1B1, SULT2B1,UGT1A1,UGT2B28
A500			
ILK Signaling	1.9E-04	-2.3	ACTB,ACTN2,JUN,MYH1,MYH2,MYH3,MYH6,MYH7, MYH8,MYL1,MYL2,MYL3

 doi:10.20944/preprints202403.1345.v1

Apelin Cardiomyocyte Signaling Pathway	2.6E-03	-2.6	ATP2A1,MYL1,MYL2,MYL3,MYLPF,PLCL2,SLC9A2
Actin Cytoskeleton Signaling	1.4E-05	-2.7	ACTB,ACTN2,APC,MPRIP,MYH1,MYH2,MYH3,MYH6, MYH7,MYH8,MYL1,MYL2,MYL3,MYLPF,TTN

Table 4. Results from upstream regulator analysis using the IPA software. Four upstream regulators were obtained, EFNA2 in the Y500 group, let-7 in and IGF1 in the A50 group and MYOCD in the 500 kBq group.

Upstream regulator	Molecule type	p	z	Target molecules in dataset
Y500				
EFNA2	kinase	4.5E-03	2.0	KRT13,KRT4,PKP1,TGM1
A50				
let-7	microRNA	2.3E-02	2.2	APC,BOP1,IGF1R,MYD88,STARD13
IGF1	growth factor	2.0E-03	-2.2	GFAP,IGF1R,IGFBP3,PSMB8,SLC20A1
A500				
MYOCD	transcription regulator	7.8E-10	-2.1	ACTN2,CASQ2,CNN1,COL1A1,HSPB7,MYH6,MYH7,MYL2,TNNC1,TNNI1,TTN

3.5. Histological Evaluation of Rat Thyroid Tissue

Individual thyroid tissue samples were morphologically evaluated for each rat. In the Y50 group 3/6, Y500 group 2/6, A50 group 1/6 and A500 3/6 had neoplastic changes, respectively. In the young control group 4/6 and in the adult control group 3/6 had neoplastic changes.

4. Discussion

In the present study, we investigated late age- and dose-related effects of ^{131}I exposure on protein expression in thyroid tissue of young and adult rats twelve months after injection. In total, 7147 proteins were quantified, of them 1,799 proteins were significantly regulated, of which 758 were unique for only one of the exposed groups and the remaining 1,041 proteins were seen in at least two of the exposed groups. Several canonical pathways were thereby identified using these 1,799 proteins in the IPA analysis. Furthermore, different types of biomarker candidates related to ^{131}I exposure, age, absorbed dose, and thyroid function and thyroid cancer were proposed.

Ideally, a suitable biomarker candidate should preferably have increased expression, since it is technically easier to analyse compared to decreased expression, especially when using conventional protein detection methods such as Western blotting or ELISA. To be able to use down-regulated biomarkers, the expression levels needs to be sufficiently low compared to normal expression to be technically detectable. More specifically, exposure-related biomarkers should be present in all groups, age-related biomarkers should only be present in young or adult individuals, and dose-related biomarkers should only be present in the 50 or 500 kBq groups. The unique biomarkers are only present in one of the groups (Y50, Y500, A50 or A500), which could be used to propose combined age- and dose-dependent biomarker candidates.

When evaluating the 24 common proteins identified in all groups in the present study as potential exposure-related biomarkers, no single protein had increased expression in all four test groups; 23 of the proteins were under-expressed in all groups, and the TIMELESS protein was under-expressed in all groups except the A500 group. All of these down-regulated proteins had low protein expression levels (log2 ratio -0.58-(-1.5)). Thus, none of these proteins would be suitable as biomarkers. Furthermore, none of these proteins have, as far as we know, previously been proposed as potential biodosimeters [25].

The aldehyde dehydrogenase family 1, subfamily A7 (ALDH1A7), apolipoprotein B mRNA editing enzyme catalytic subunit 2 (APOBEC2), ATP synthase C subunit lysine N-methyltransferase

 doi:10.20944/preprints202403.1345.v1

(ATPSCKMT), immunoglobulin heavy constant gamma (IGHG), lipocalin 2 (LCN2), galectin-5 (LGALS5), proline rich 33 (PRR33), proteasome 20S subunit beta 8 (PSMB8), one of the heterogeneous ribonucleoparticle complexes A1b (RT1-A1B), and type IV pilus assembly (TAPC2) proteins were over-expressed in adult rats (log2 ratio 0.58-4.5), and were age-related, dose independent biomarker candidates. In young rats, no protein with increased expression levels was seen in both the Y50 and Y500 groups and the expression level of the down-regulated proteins was too low to be considered as suitable biomarker candidates (log2 ratio -0.58-(-1)). Previously, the LCN2 protein was suggested as a diagnostic biomarker for well differentiated thyroid cancer including PTC (increased expression in thyroid cancer tissue both in children and adults and in plasma in children) [26–29]. Interestingly, increased LNC2 expression was not shown in young rats in the present study, possibly due to translational effects related to biological differences between rats and humans.

Here, we propose the NME/NM23 nucleoside diphosphate kinase 3 (NME3) and paralemmin 2 (PALM2) (50kBqgroups, log2 ratio 0.58-2) and chloride channel CLIC like 1 (CLCC1), carnitine palmitoyl transferase 2 (CPT2) and haptoglobin (HP) (500 kBq groups, log2 ratio 0.58-1.5) proteins as dose-related and age independent candidate biomarkers with increased expression. Of these proteins, HP protein levels in serum were related to thyroid hormone levels, with increased expression levels in patients with hyperthyroidism and thyroid cancer, and reduced at hypothyroidism [30,31]. The down-regulated dose-related and age independent proteins in the present study had too low fold change to be considered as biomarker candidates.

If single biomarkers are not available or suitable, a panel of unique proteins with increased expression, for each age and activity level (Y50, Y500, A50 and A500) can be used both for age- and dose- dependence. One suggestion of such a panel is to include the top ten proteins uniquely expressed for each of the four groups, with the highest increased expression (altogether 40 proteins). Several of the proposed biomarkers have previously been identified in thyroid diseases. Increased beta-2-microglobulin (*B2M*) expression was seen in thyroid cancer [32–34]. Increased enzymatic activity of ADA was seen for thyrotoxicosis, thyroid cancer, adenomas and thyroiditis [35]. Aberrant methylation patterns for serpin family B member 5 (*SERPINB5*) (together with *TIMP3*, *RARB2*, *RASSF1*, *TPO* and *TSHR*) were used to distinguish between papillary thyroid cancer (PTC) and normal thyroid tissue [36]. Increased sphingomyelin phosphodiesterase 1 (SMPD1) protein expression was related to aging and thyroid cancer in mice [37]. Increased BAG cochaperone 5 (BAG5) (together with FN1) protein expression was correlated with increased PTC invasiveness [38]. The tyrosine kinase with immunoglobulin like and EGF like domains (TIE1) protein has been suggested to be involved in the early progression of PTC [39]. The S100A9 protein has an increased expression in serum for patients with autoimmune thyroiditis [40]. Increased expression of the S100 calcium binding protein A9 (S100A9) protein is uncommon in well differentiated thyroid cancers, but related to poorly differentiated types, *e.g.,* anaplastic thyroid cancer [41,42].

When comparing our present findings with those from our previous studies on similar types of rats at earlier time points (24 hours, and 3, 6, and 9 months), none of the previously suggested protein biomarkers were seen in the present study [20,43,44]. However, the thyroid hormone metabolism signalling pathway, has previously been seen using the IPA software at 24 h post irradiation for similar dose levels [17]. This might be due to differences between the studies regarding time point. Another explanation is the use of individual samples in the present study, while pooled samples were used in the previous experiments. When irradiating with low-intermediate absorbed doses (few particles hit each cell), the impact on individual cells in various organs can vary, and thus the proteomics expression may be different for each individual.

Furthermore, the biliverdin reductase A (BLVRA; Y500), haptoglobin (HP; 500 and A500), orosomucoid 1 (ORM1; A500), retinoblastoma transcriptional corepressor 1 (RB1; A50 and A500), ribosomal protein S6 kinase A1 (RPS6KA1; A500) and, mitogen-activated protein kinase 2 (MAP2K2; A50) proteins were previously suggested as radiation biodosimeters [45]. It should be noted that the proposed biodosimeters were mainly identified based on results from *in vitro* and *in vivo* studies using various cell types and usually after much higher absorbed doses than in the present study. The present study addressed low and moderate absorbed doses to the thyroid in an *in vivo* setting, where

 doi:10.20944/preprints202403.1345.v1

also non-targeted effects due to exposure of other tissues in the body, as well as thyroid hormone-related effects may be included [25].

From the IPA analysis for young rats, several of the canonical pathways were related to deregulation of hormones serotonin and melanin, and nicotine, bupropion and acetone. Furthermore, pathways related to metabolism were affected, including thyroid hormone metabolism in both groups (Y50 and Y500). Signalling pathways related to synthesis were also identified, *e.g.* gluconeogenesis, and stearate, bile acid, retinoale and cholesterol biosynthesis. The xenobiotic metabolism CAR signalling pathway was found in the A50 group. Previous studies showed that CAR receptor activation by hepatic drug metabolizing enzymes are positively correlated with increased serum TSH levels and thyroid cell proliferation [46]. IKL signalling, apelin cardiomyocyte signalling pathway and actin cytoskeleton signalling were seen in the A500 group. The apelin receptor is important for development and function of heart muscles [47].The ILK protein is involved in the actin cytoskeleton function (involved in cellular motion and maintenance of the cell structure), and ILK inhibition may cause proliferative defects, and induce cell-cycle arrest and apoptosis [48].

Four upstream regulators were detected in the IPA analysis, i.e. EFNA2 (Y500), Let-7 and IGF1 (A50), and MYOCD (A500). The EFNA2 protein is a member of the Ephrin family and is a receptor tyrosine kinase that is important for development, in particular of the nervous system [47]**.** This protein is located in the plasma membrane and interacts with the keratin 13 (KRT13), keratin 4 (KRT4), plakophilin-1 (PKP1) and transglutaminase-1 (TGM1) proteins [47], and none of them have to our knowledge been connected to thyroid gland or thyroid cancer. The Let-7 micoRNA is involved in suppression of the RAS oncogene leading to suppression of PTC development [49]**.** The Let-7 upstream regulator interacts with the adenomatous polyposis coli (APC), insulin-like growth factor 1 receptor (IGF1R) and myeloid differentiation primary response 88 (MYD88) proteins, and has a direct contact with the block of proliferation 1 ribosomal biogenesis factor (BOP1) and StAR-related lipid transfer domain protein 13 (STARD13) [47]. Mutations in the APC gene is found in patients with familial adenomatous polyposis, which may manifest also in PTC in a few of these patients [50–52]. MYD88 has been related to thyroid dysfunction and FTC [53–56]. BOP1 and STARD13 are not related to thyroid function. The IGF1 protein functions similarly to insulin, but promotes growth to a larger extent [47]. The IGF1 upstream regulator (inhibition) interacts with glial fibrillary acidic protein (GFAP), proteasome 20S subunit beta 8 (PSMB8) and solute carrier family 20 member 1 (SLC20A1), and a direct contact with insulin like growth factor 1 receptor (IGF1R) and insulin like growth factor binding protein 3 (IGFBP3) [47]. No previous association with thyroid function was seen for GFAP. PSMB8 has been suggested as a target for the miR-451a, which is a biomarker candidate for PTC [57]. Elevated serum levels and thyroid tissue expression of IGF1R is associated with PTC and ATC [58,59] . IGFBP3 is suggested to affect the prognosis and induction of lymph node metastasis in PTC, but decreased serum levels of IGFBP3 is associated with hypothyroidism, and elevated levels with hyperthyroidism [60–62]. MYOCD is a nuclear protein and transcription factor that is highly expressed in heart and smooth muscles [47]. The MYOCD upstream regulator (inhibition) is located in the nucleus and influences the actinin alpha 2 (ACTN2), calsequestrin 2 (CASQ2), calponin 1 (CNN1), collagen type I alpha 1 chain (COL1A1), heat shock protein family b (small) member 7 (HSPB7), myosin heavy chain 6 (MYH6), myosin heavy chain 7 (MYH7), myosin light chain 2 (MYL2), troponin c1, slow skeletal and cardiac type (TNNC1), troponin I1, slow skeletal type (TNNI1), and titin (TTN) proteins by expression. No previous association with thyroid disease were seen for CNN1, MYH6, MYH7, MYL2, TNNC1, TNNI1 or TNN. Increased expression of CASQ2 in thyroid tissue is correlated to Graves ophthalmopathy [63]. *COL1A1* gene expression is seen for PTC, and relates to the progression of these tumours [64,65]].

When evaluating the morphology of the thyroid tissue, neoplastic changes were seen for about half of the individuals in all of the groups except the A50 group, where one abnormal sample was identified. It should be noted that the morphological and proteomic analyses were made on different parts of the thyroid samples. However, to fully evaluate any potential cancer induction longer follow-up time had been needed. Previous studies have shown that the thyroid morphology changes with age in Sprague Dawley rats [22]. Furthermore, the result in the present study is in consistency with

 doi:10.20944/preprints202403.1345.v1

the results from screening of 360,000 children in the Fukushima region, where about 200 thyroid cancer cases were found [66]. The estimated absorbed dose the thyroid was low (20 mGy) and these cases are most probably a result of detailed high resolution ultrasonography screening. When similar examinations were done in age matched children living in three other areas of Japan the incidence of thyroid nodules and cysts were in the same range as for the children exposed at the Fukushima accident [67]. It is thus probable that the morphological changes found in children in Japan and in our study are sporadic changes, not depending on radiation exposure.

5. Conclusion

In the present study, long–term proteomic effects were investigated in young and adult rats for exposure of low activities of ^{131}I (50-500 kBq). Several biomarker candidates are proposed for ^{131}I exposure, age, many of which are known to be related to thyroid function or thyroid cancer. A panel of 40 proteins for ^{131}I exposure, dose-related biomarker candidates, and age-related biomarker candidates, are suggested. These potential biomarkers need to be validated before being implemented in clinical or radiation protection-related practice.

Several Ingenuity canonical pathways were obtained for young rats and could be categorised into hormone regulation, metabolism and synthesis. In the adult rats signalling pathways were related to TSH levels and thyroid cell proliferation.

Supplementary Materials: The following supporting information can be downloaded at the website of this paper posted on Preprints.org.

Author Contributions: Conceptualization: MD, ES, JS, BL and EFA. **Methodology:** MD, EB, ES, JS, TZP, BL, KH and EFA. **Validation:** MD, KH and EFA. **Formal analysis:** MD, EB, JS, TZP, BL and CY. **Investigation:** MD, ES, JS, TZP and BL. **Resources:** MD, ES, JS, TZP, BL, KH and EFA. **Data curation:** MD and EB. **Writing – original draft:** MD. **Writing – review & editing:** MD, ES, JS, TZP, BL, CY, EB, KH and EFA. **Visualization:** MD, JS, TZP, BL, KH and EFA. **Supervision:** KH and EFA. **Project administration:** KH and EFA. **Funding acquisition:** MD and EFA.

Funding: This study was supported by grants from BioCARE – a National Strategic Research Program at the University of Gothenburg, the Swedish Cancer Society (grant no. 3427), the Swedish Research Council (grant no. 21073), the Swedish state under the agreement between the Swedish government and the county councils – the ALF-agreement (ALFGBG-725031), Swedish Radiation Safety Authority (SSM), the King Gustav V Jubilee Clinic Cancer Research Foundation, the Sahlgrenska University Hospital Research Funds, the Assar Gabrielsson Cancer Research Foundation, the Adlerbertska Research Foundation, the Knut and Alice Wallenberg Foundation, the Royal Society of Arts and Sciences in Gothenburg (KVVS), and the Wilhelm and Martina Lundgren Research Foundation.

Acknowledgments: Quantitative proteomics analysis was performed at the Proteomics Core Facility at Sahlgrenska Academy, University of Gothenburg. The Proteomics Core Facility is grateful to the Inga-Britt and Arne Lundberg Research Foundation for the donation of the Orbitrap Fusion Tribrid MS instrument. Authors also thank Daniella Pettersson and Amin Al-Awar for help with haematoxylin and eosin staining of the tissue sections and the certified pathologist Dr. Ghayeb Mohammad at Sahlgrenska University Hospital for evaluation of the tissue sections.

Conflicts of Interest: The authors have no competing interest to declare.

Ethical Permission: This animal experiment was approved by the Ethical Committee on Animal Experiments in Gothenburg, Sweden (Permit Number: 146-2015)

References

1. Nussey S, Whitehead S. Endocrinology: An Integrated Approach. Oxford2001.
2. Raymond J, LaFranchi SH. Fetal and neonatal thyroid function: review and summary of significant new findings. Curr Opin Endocrinol Diabetes Obes. 2010;17(1):1-7.
3. Mullur R, Liu YY, Brent GA. Thyroid hormone regulation of metabolism. Physiol Rev. 2014;94(2):355-82.
4. Srikantia N, Rishi KS, Janaki MG, Bilimagga RS, Ponni A, Rajeev AG, et al. How common is hypothyroidism after external radiotherapy to neck in head and neck cancer patients? Indian journal of

 doi:10.20944/preprints202403.1345.v1

medical and paediatric oncology : official journal of Indian Society of Medical & Paediatric Oncology. 2011;32(3):143-8.
5. Holm LE. Thyroid cancer after exposure to radioiodine. Strahlenschutz Forsch Prax. 1985;25:36-56.
6. DeGroot LJ. Effects of irradiation on the thyroid gland. Endocrinol Metab Clin North Am. 1993;22(3):607-15.
7. Inskip PD. Thyroid cancer after radiotherapy for childhood cancer. Med Pediatr Oncol. 2001;36(5):568-73.
8. Robbins J, Schneider AB. Radioiodine-induced thyroid cancer: Studies in the aftermath of the accident at Chernobyl. Trends Endocrinol Metab. 1998;9(3):87-94.
9. Ron E, Lubin JH, Shore RE, Mabuchi K, Modan B, Pottern LM, et al. Thyroid cancer after exposure to external radiation: a pooled analysis of seven studies. Radiat Res. 1995;141(3):259-77.
10. Weiss W. Chernobyl Thyroid Cancer: 30 Years of Follow-up Overview. Radiat Prot Dosimetry. 2018;182(1):58-61.
11. IAEA CF. Chernobyl's legacy: health, environmental and socio-economic impacts and recommendations to the governments of Belarus, the Russian Federation and Ukraine. 2005.
12. Zablotska LB, Ron E, Rozhko AV, Hatch M, Polyanskaya ON, Brenner AV, et al. Thyroid cancer risk in Belarus among children and adolescents exposed to radioiodine after the Chornobyl accident. Br J Cancer. 2011;104(1):181-7.
13. Tronko MD, Howe GR, Bogdanova TI, Bouville AC, Epstein OV, Brill AB, et al. A cohort study of thyroid cancer and other thyroid diseases after the chornobyl accident: thyroid cancer in Ukraine detected during first screening. J Natl Cancer Inst. 2006;98(13):897-903.
14. Amundson SA, Fornace AJ, Jr. Gene expression profiles for monitoring radiation exposure. Radiat Prot Dosimetry. 2001;97(1):11-6.
15. Chin RI, Wu FS, Menda Y, Kim H. Radiopharmaceuticals for Neuroendocrine Tumors. Semin Radiat Oncol. 2021;31(1):60-70.
16. Chaudhry MA. Biomarkers for human radiation exposure. J Biomed Sci. 2008;15(5):557-63.
17. Rudqvist N, Spetz J, Schuler E, Parris TZ, Langen B, Helou K, et al. Transcriptional response to 131I exposure of rat thyroid gland. PLoS One. 2017;12(2):e0171797.
18. Rudqvist N, Schuler E, Parris TZ, Langen B, Helou K, Forssell-Aronsson E. Dose-specific transcriptional responses in thyroid tissue in mice after (131)I administration. Nucl Med Biol. 2015;42(3):263-8.
19. Langen B, Rudqvist N, Parris TZ, Helou K, Forssell-Aronsson E. Circadian rhythm influences genome-wide transcriptional responses to (131)I in a tissue-specific manner in mice. EJNMMI Res. 2015;5(1):75.
20. Larsson M, Rudqvist N, Spetz J, Shubbar E, Parris TZ, Langen B, et al. Long-term transcriptomic and proteomic effects in Sprague Dawley rat thyroid and plasma after internal low dose 131I exposure. PLoS One. 2020;15(12):e0244098.
21. Spetz J, Rudqvist N, Forssell-Aronsson E. Biodistribution and dosimetry of free 211At, 125I- and 131I- in rats. Cancer Biother Radiopharm. 2013;28(9):657-64.
22. Rao-Rupanagudi S, Heywood R, Gopinath C. Age-related changes in thyroid structure and function in Sprague-Dawley rats. Vet Pathol. 1992;29(4):278-87.
23. Wisniewski JR, Zougman A, Nagaraj N, Mann M. Universal sample preparation method for proteome analysis. Nat Methods. 2009;6(5):359-62.
24. Perez-Riverol Y, Csordas A, Bai J, Bernal-Llinares M, Hewapathirana S, Kundu DJ, et al. The PRIDE database and related tools and resources in 2019: improving support for quantification data. Nucleic Acids Res. 2019;47(D1):D442-D50.
25. Langen B, Rudqvist N, Parris TZ, Schuler E, Helou K, Forssell-Aronsson E. Comparative analysis of transcriptional gene regulation indicates similar physiologic response in mouse tissues at low absorbed doses from intravenously administered 211At. J Nucl Med. 2013;54(6):990-8.
26. Celestino R, Nome T, Pestana A, Hoff AM, Goncalves AP, Pereira L, et al. CRABP1, C1QL1 and LCN2 are biomarkers of differentiated thyroid carcinoma, and predict extrathyroidal extension. BMC Cancer. 2018;18(1):68.
27. Tai J, Wang S, Zhang J, Ge W, Liu Y, Li X, et al. Up-regulated lipocalin-2 in pediatric thyroid cancer correlated with poor clinical characteristics. Eur Arch Otorhinolaryngol. 2018;275(11):2823-8.
28. Rosignolo F, Sponziello M, Durante C, Puppin C, Mio C, Baldan F, et al. Expression of PAX8 Target Genes in Papillary Thyroid Carcinoma. PLoS One. 2016;11(6):e0156658.
29. Ma H, Xu S, Yan J, Zhang C, Qin S, Wang X, et al. The value of tumor markers in the diagnosis of papillary thyroid carcinoma alone and in combination. Pol J Pathol. 2014;65(3):202-9.
30. Ghoshal A, Garmo H, Arthur R, Carroll P, Holmberg L, Hammar N, et al. Thyroid cancer risk in the Swedish AMORIS study: the role of inflammatory biomarkers in serum. Oncotarget. 2018;9(1):774-82.
31. Fan Y, Shi L, Liu Q, Dong R, Zhang Q, Yang S, et al. Discovery and identification of potential biomarkers of papillary thyroid carcinoma. Mol Cancer. 2009;8:79.

 doi:10.20944/preprints202403.1345.v1

32. Mitteldorf CA, de Sousa-Canavez JM, Massumoto C, da Camara-Lopes LH. Fine-needle aspiration biopsy of thyroid nodules as a possible source for molecular studies: analysis of RNA obtained from routine cases. Diagn Cytopathol. 2008;36(12):899-903.
33. Weber R, Bertoni AP, Bessestil LW, Brasil BM, Brum LS, Furlanetto TW. Validation of reference genes for normalization gene expression in reverse transcription quantitative PCR in human normal thyroid and goiter tissue. Biomed Res Int. 2014;2014:198582.
34. Razavi SA, Afsharpad M, Modarressi MH, Zarkesh M, Yaghmaei P, Nasiri S, et al. Validation of Reference Genes for Normalization of Relative qRT-PCR Studies in Papillary Thyroid Carcinoma. Sci Rep. 2019;9(1):15241.
35. Goldberg DM, Goudie RB. Nucleases and adenosine deaminase in malignant and non-malignant lesions of the human thyroid. Br J Cancer. 1968;22(2):220-36.
36. Stephen JK, Chen KM, Merritt J, Chitale D, Divine G, Worsham MJ. Methylation markers differentiate thyroid cancer from benign nodules. J Endocrinol Invest. 2018;41(2):163-70.
37. Traina G, Cataldi S, Siccu P, Loreti E, Ferri I, Sidoni A, et al. Mouse Thyroid Gland Changes in Aging: Implication of Galectin-3 and Sphingomyelinase. Mediators Inflamm. 2017;2017:8102170.
38. Zhang DL, Wang JM, Wu T, Du X, Yan J, Du ZX, et al. BAG5 promotes invasion of papillary thyroid cancer cells via upregulation of fibronectin 1 at the translational level. Biochim Biophys Acta Mol Cell Res. 2020;1867(9):118715.
39. Ito Y, Yoshida H, Uruno T, Nakano K, Takamura Y, Miya A, et al. Tie-1 tyrosine kinase expression in human thyroid neoplasms. Histopathology. 2004;44(4):318-22.
40. Korkmaz H, Tabur S, Savas E, Ozkaya M, Aksoy SN, Aksoy N, et al. Evaluation of Serum S100A8/S100A9 Levels in Patients with Autoimmune Thyroid Diseases. Balkan Med J. 2016;33(5):547-51.
41. Ito Y, Arai K, Nozawa R, Yoshida H, Hirokawa M, Fukushima M, et al. S100A8 and S100A9 expression is a crucial factor for dedifferentiation in thyroid carcinoma. Anticancer Res. 2009;29(10):4157-61.
42. Ito Y, Arai K, Ryushi, Nozawa, Yoshida H, Tomoda C, et al. S100A9 expression is significantly linked to dedifferentiation of thyroid carcinoma. Pathol Res Pract. 2005;201(8-9):551-6.
43. Rudqvist N. Radiobiological Effects of the Thyroid Gland. https://gupea.ub.gu.se/bitstream/2077/38006/1/gupea_2077_38006_1.pdf: University of Gothenburg; 2015.
44. Larsson M. RN, Spetz J., Shubbar E. , Parris TZ., Langen B., Helou K., Forssell-Aronsson E. Age related long-term response in rat thyroid tissue and plasma after internal low dose exposure to 131I 2021.
45. Marchetti F, Coleman MA, Jones IM, Wyrobek AJ. Candidate protein biodosimeters of human exposure to ionizing radiation. Int J Radiat Biol. 2006;82(9):605-39.
46. Qatanani M, Zhang J, Moore DD. Role of the constitutive androstane receptor in xenobiotic-induced thyroid hormone metabolism. Endocrinology. 2005;146(3):995-1002.
47. Stelzer G, Rosen N, Plaschkes I, Zimmerman S, Twik M, Fishilevich S, et al. The GeneCards Suite: From Gene Data Mining to Disease Genome Sequence Analyses. Curr Protoc Bioinformatics. 2016;54:1 30 1-1 3.
48. Yen CF, Wang HS, Lee CL, Liao SK. Roles of integrin-linked kinase in cell signaling and its perspectives as a therapeutic target. Gynecology and Minimally Invasive Therapy. 2014;3(3):67-72.
49. Perdas E, Stawski R, Nowak D, Zubrzycka M. The Role of miRNA in Papillary Thyroid Cancer in the Context of miRNA Let-7 Family. Int J Mol Sci. 2016;17(6).
50. Nieminen TT, Walker CJ, Olkinuora A, Genutis LK, O'Malley M, Wakely PE, et al. Thyroid Carcinomas That Occur in Familial Adenomatous Polyposis Patients Recurrently Harbor Somatic Variants in APC, BRAF, and KTM2D. Thyroid. 2020;30(3):380-8.
51. Akaishi J, Kondo T, Sugino K, Ogimi Y, Masaki C, Hames KY, et al. Cribriform-Morular Variant of Papillary Thyroid Carcinoma: Clinical and Pathological Features of 30 Cases. World J Surg. 2018;42(11):3616-23.
52. Cetta F, Montalto G, Gori M, Curia MC, Cama A, Olschwang S. Germline mutations of the APC gene in patients with familial adenomatous polyposis-associated thyroid carcinoma: results from a European cooperative study. J Clin Endocrinol Metab. 2000;85(1):286-92.
53. Li C, Peng S, Liu X, Han C, Wang X, Jin T, et al. Glycyrrhizin, a Direct HMGB1 Antagonist, Ameliorates Inflammatory Infiltration in a Model of Autoimmune Thyroiditis via Inhibition of TLR2-HMGB1 Signaling. Thyroid. 2017;27(5):722-31.
54. Peng S, Li C, Wang X, Liu X, Han C, Jin T, et al. Increased Toll-Like Receptors Activity and TLR Ligands in Patients with Autoimmune Thyroid Diseases. Front Immunol. 2016;7:578.
55. Jacques C, Guillotin D, Fontaine JF, Franc B, Mirebeau-Prunier D, Fleury A, et al. DNA microarray and miRNA analyses reinforce the classification of follicular thyroid tumors. J Clin Endocrinol Metab. 2013;98(5):E981-9.
56. Rocchi R, Kimura H, Tzou SC, Suzuki K, Rose NR, Pinchera A, et al. Toll-like receptor-MyD88 and Fc receptor pathways of mast cells mediate the thyroid dysfunctions observed during nonthyroidal illness. Proc Natl Acad Sci U S A. 2007;104(14):6019-24.
57. Fan X, Zhao Y. miR-451a inhibits cancer growth, epithelial-mesenchymal transition and induces apoptosis in papillary thyroid cancer by targeting PSMB8. J Cell Mol Med. 2019;23(12):8067-75.

 doi:10.20944/preprints202403.1345.v1

58. Lawnicka H, Motylewska E, Borkowska M, Kuzdak K, Siejka A, Swietoslawski J, et al. Elevated serum concentrations of IGF-1 and IGF-1R in patients with thyroid cancers. Biomed Pap Med Fac Univ Palacky Olomouc Czech Repub. 2020;164(1):77-83.
59. He L, Zhang S, Zhang X, Liu R, Guan H, Zhang H. Effects of insulin analogs and glucagon-like peptide-1 receptor agonists on proliferation and cellular energy metabolism in papillary thyroid cancer. Onco Targets Ther. 2017;10:5621-31.
60. Huang Y, Chang A, Zhou W, Zhao H, Zhuo X. IGFBP3 as an indicator of lymph node metastasis and unfavorable prognosis for papillary thyroid carcinoma. Clin Exp Med. 2020;20(4):515-25.
61. Iglesias P, Bayon C, Mendez J, Gancedo PG, Grande C, Diez JJ. Serum insulin-like growth factor type 1, insulin-like growth factor-binding protein-1, and insulin-like growth factor-binding protein-3 concentrations in patients with thyroid dysfunction. Thyroid. 2001;11(11):1043-8.
62. Lakatos P, Foldes J, Nagy Z, Takacs I, Speer G, Horvath C, et al. Serum insulin-like growth factor-I, insulin-like growth factor binding proteins, and bone mineral content in hyperthyroidism. Thyroid. 2000;10(5):417-23.
63. Wescombe L, Lahooti H, Gopinath B, Wall JR. The cardiac calsequestrin gene (CASQ2) is up-regulated in the thyroid in patients with Graves' ophthalmopathy--support for a role of autoimmunity against calsequestrin as the triggering event. Clin Endocrinol (Oxf). 2010;73(4):522-8.
64. Liang W, Sun F. Identification of key genes of papillary thyroid cancer using integrated bioinformatics analysis. J Endocrinol Invest. 2018;41(10):1237-45.
65. Huang C, Yang X, Han L, Fan Z, Liu B, Zhang C, et al. The prognostic potential of alpha-1 type I collagen expression in papillary thyroid cancer. Biochem Biophys Res Commun. 2019;515(1):125-32.
66. Yamashita S, Suzuki S, Suzuki S, Shimura H, Saenko V. Lessons from Fukushima: Latest Findings of Thyroid Cancer After the Fukushima Nuclear Power Plant Accident. Thyroid. 2018;28(1):11-22.
67. Hayashida N, Imaizumi M, Shimura H, Okubo N, Asari Y, Nigawara T, et al. Thyroid ultrasound findings in children from three Japanese prefectures: Aomori, Yamanashi and Nagasaki. PLoS One. 2013;8(12):e83220.